

Low-Resistance Spin-Dependent Tunnel Junctions With HfAlO_x Barriers for High-Density Recording-Head Application

Jianguo Wang, *Member, IEEE*, P. P. Freitas, E. Snoeck, X. Batlle, and J. Cuadra

Abstract—Spin-dependent tunnel junctions with the structure (Ta 70 Å/NiFe 70 Å/MnIr 80 Å/CoFe 35 Å/HfAlO_x/CoFe 35 Å/NiFe 40 Å/TiW(N) 150 Å) were fabricated on top of 600-Å-thick ion-beam-smoothed low-resistance Al electrodes. HfAlO_x barriers were formed by natural oxidation (5 min at 1 torr in pure O₂) of 5-Å-thick (2-Å Hf + 3-Å Al) films or 6-Å-thick (2-Å Hf + 4-Å Al) films. Resistance \times area ($R \times A$) products of $0.65 \Omega \times \mu^2$ and $2.1 \Omega \times \mu\text{m}^2$ were achieved with 9.5% and 13.5% tunnel magnetoresistance signal (TMR), respectively. Current inhomogeneity effects on the measured ($R \times A$) products and TMR values were calculated in particular for junctions with resistance below $1 \Omega \times \mu\text{m}^2$. Transmission electron microscopy indicates that HfAlO_x forms a continuous amorphous barrier that follows conformally the topography of the bottom electrode. X-ray photoelectron spectroscopy analysis indicates that 2.5% metallic Hf is left inside the barrier closer to the bottom electrode. These low-resistance tunnel junctions are attractive for read-head applications at recording densities above 100 Gbit/in².

Index Terms—Magnetoresistive materials and devices, read heads, tunnel junction.

I. INTRODUCTION

LOW-RESISTANCE spin-dependent tunnel junctions (as well as current-perpendicular-to-plane GMR sensors) are possible candidates for replacement of current-in-plane spin-valve sensors in reads heads as recording densities move beyond 100 Gbit/in². For proper signal-to-noise ratio, and for compatibility with head preamps, tunnel junctions must have very low resistance ($<1 \Omega \times \mu\text{m}^2$) and maintain reasonably large tunnel magnetoresistance (TMR). Results from various groups on low-resistance junctions using naturally oxidized AlO_x barriers (5–7 Å Al) report resistance \times area ($R \times A$) products ranging from 3–20 $\Omega \times \mu\text{m}^2$, but with TMR values scaled down to 10%–20% [1]–[4]. Another approach to producing low-resistance junctions is to use lower bandgap oxides (ZrO_x, ZrAlO_x, and HfAlO_x, among others). Junctions with

a (2.5 Å Zr + 4.5 Å Al)O_x barrier were shown to have low resistance (5–9 $\Omega \times \mu\text{m}^2$) with TMR values reaching 15.3% [5]. This paper describes the properties of low-resistance ($0.65 \Omega \times \mu\text{m}^2$ – $2.1 \Omega \times \mu\text{m}^2$) amorphous HfAlO_x barriers, with TMR values reaching 9.5%–13.5%. For these low junction resistances, care must be taken to take into account current inhomogeneity across the barrier in the interpretation of measured transport properties.

II. EXPERIMENT

The junctions used in this work have the structure, glass/bottom lead/Ta 70 Å/NiFe 70 Å/MnIr 80 Å/CoFe 35 Å/HfAlO_x/CoFe 35 Å/NiFe 40 Å/TiW(N) 150 Å/top lead. NiFe, CoFe, and MnIr here stand for Ni₈₁Fe₁₉, Co₉₀Fe₁₀, and Mn₈₃Ir₁₇, respectively. Except for the bottom and top leads, and the Ti₁₀W₉₀ (N) antireflective coating (ARC), all layers were deposited by dc magnetron sputtering in a Nordiko 2000 sputtering system, with a base pressure of 5×10^{-8} torr. During deposition, a magnetic field of 20 Oe was applied to induce parallel easy axis in the bottom and top magnetic layers. The HfAlO_x is grown by depositing sequentially Hf (2 Å) and Al (3, 4 Å), followed by moving the sample to the loadlock and oxidizing under a controlled oxygen atmosphere (1 torr for 5 min). The bottom and top leads and the ARC layer were deposited by magnetron sputtering in a Nordiko 7000 cluster system (base pressure 5×10^{-9} torr). The bottom lead is formed by 600 Å of Al, 1% Si, and 0.5% Cu (0.6 Ohm/sq), subject to a postdeposition anneal at 400 °C for 30 min. The Al–Si–Cu layer is then ion beam smoothed for 90 s at a substrate pan of 40°, leading to an antiferromagnetic root-mean-square roughness less than 2 Å. The micrometer-size junctions were patterned by a self-aligned microfabrication process using direct-write laser-lithography and ion-beam milling. Junctions were measured using a four-probe dc method. Anneals were carried out in a vacuum furnace (10^{-6} torr) under a 3000-Oe magnetic field for 40 min, with ramp-up and cool-down times of about 1 h. The structural characterization of the junctions was made by transmission electron microscopy (TEM) on cross-sectional specimens. The specimens were glued face to face, mechanically polished, then ion milled to achieve electron transparency. The TEM experiments were carried out on a Philips CM30 microscope whose point resolution is 0.19 nm. X-ray photoelectron spectroscopy (XPS) analysis was made in specially fabricated specimens allowing the separation of the different peaks requiring study (Hf, Al, Co, Fe, and their oxides in the barrier region).

Manuscript received February 13, 2002; revised May 22, 2002. This work was supported by Project 34116/99 from FCT-Portugal and by Seagate. J. Wang was supported by PRAXIS/BD/15572/98 Ph.D. Grant. X. Batlle and J. Cuadra were supported by Spanish CICYT and Catalan DURSI.

J. Wang and P. P. Freitas are with the Instituto de Engenharia de Sistemas e Computadores (INESC), 1000-029 Lisbon, Portugal and also with the Instituto Superior Tecnico (IST), Physics Department, 1096 Lisbon, Portugal (e-mail: jianguo.wang@inesc.pt).

E. Snoeck is with the Centre d'Elaboration de Matériaux et d'Etudes Structurales (CEMES-CNRS), F-31055 Toulouse Cedex, France.

X. Batlle and J. Cuadra are with the Departamento de Física Fundamental, Universitat de Barcelona, Catalonia, Spain.

Digital Object Identifier 10.1109/TMAG.2002.803175.

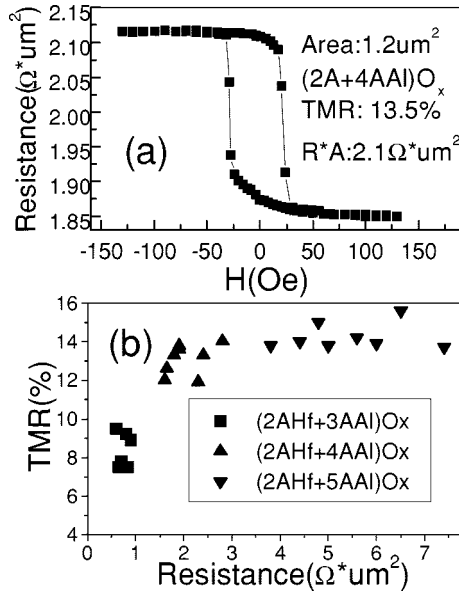


Fig. 1. (a) Resistance loop after annealing at 240 °C for 40 min for a junction with the (2-Å Hf + 4-Å Al) + oxide barrier. (b) TMR versus resistance area of junctions with a different barrier.

III. RESULTS AND DISCUSSION

Fig. 1(a) shows the measured resistance loop of the $HfAlO_x$ junction, where the barrier was formed by natural oxidation of a (2-Å Hf + 4-Å Al) film. The junction area is $1.2 \mu m^2$. TMR of 13.5% and an $R \times A$ product of $2.1 \Omega \times \mu m^2$ were obtained. The measured breakdown voltage ($V_{\text{breakdown}}$) and the bias voltage (V_{half}) where TMR goes to half of its initial value are 458 mV and 241 mV, respectively. After fitting the I - V curves by Simmons's model, the effective barrier height and barrier thickness are 0.31 eV and 7.58 Å (these numbers are given just as indicative parameters, since this model does not apply to such thin barriers where weak spots/pinholes do occur). Fig. 1(b) shows TMR versus $R \times A$ product with different barrier junctions. For junctions with a (2-Å Hf + 4-Å Al) O_x barrier, 15% TMR is obtained with $R \times A$ product ranging from 4–7 $\Omega \times \mu m^2$. For (2-Å Hf + 3-Å Al) O_x barrier junctions, 9.5% TMR is obtained with $R \times A$ product ranging from 0.65–1.2 $\Omega \times \mu m^2$. The measured TMR and $R \times A$ product decrease with decreasing barrier thickness. All data shown in Fig. 1 refer to the measured values from a real device without correction. Four-probe measurement was used to release lead resistance contributions. Junctions are annealed at 240 °C for 40 min to set up the exchange bias field in MnIr–CoFe bilayer [6].

Due to the comparable resistance of the bottom lead and junction barrier, current flowing at the edges of the top electrode leaks to the voltage branch before flowing through the barrier (see inset cross-section model). This will affect the TMR and $R \times A$ product measured by the four-point probe method [7], when the junction $R \times A$ product is below $1 \Omega \times \mu m^2$. For our lead-junction geometry and materials (lead width is much larger than the junction width), true $R \times A$ and TMR values are approached for junction areas below $0.01 \mu m^2$. At larger junction areas, the measured $R \times A$ product increases with the junction area, while TMR decreases [8], [9]. The current

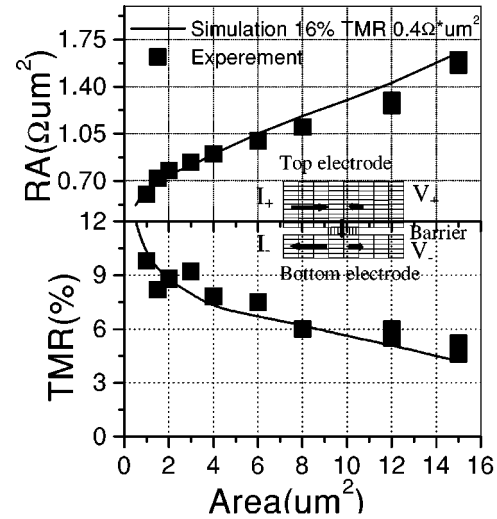


Fig. 2. $R \times A$ products and TMR values versus junction area for junctions with a (2-Å Hf + 3-Å Al) + oxide.

distribution simulation is made by using the FastHenry program [10] which is a three-dimensional (3-D) inductance extraction program, where the conductors and barrier are modeled as a 3-D resistor network (see inset cross-section model). In the simulation, the junction shape was assumed to be square, with constant cross section across junction thickness. For the simulation of the present experimental data, the resistivity of the bottom and top electrodes is $0.04 \Omega \cdot \mu m$, and the resistivity of the barrier is assumed at $500 \Omega \cdot \mu m$ in order to fit the $R \times A$ versus A (area) data. A TMR of 16% was assumed in the simulation. The width of the bottom and top leads are respectively 26 μm and 8 μm , and junction area $1 \mu m^2$ (area measured by SEM). Fig. 2 shows the experimental data and calculated $R \times A$ and TMR dependences on junction area. From the simulation, if the junction area is $0.01 \mu m^2$ ($0.1 \mu m \times 0.1 \mu m$), the measured TMR and $R \times A$ product should be 14.2% and $0.45 \Omega \times \mu m^2$ for the present material with this simulation results.

TEM was used to study these $HfAlO_x$ barriers. For this study, junctions with a (2-Å Hf + 4-Å Al) O_x barrier were analyzed. The low-resolution TEM micrograph shows that the $HfAlO_x$ barrier is continuous and follows conformally the topography of the bottom Al electrode. High-resolution TEM (Fig. 3) analyses shows the barrier to be amorphous, 10 Å thick, and with a few weak spots occurring in places where topographical defects occur already at the surface of the Al lead.

In order to clarify the oxidation status of the barrier, XPS analysis was performed in specially prepared samples, allowing the observation of the different oxide peaks. Fig. 4 shows data obtained in the structure Si/Ti 50 Å/CoFe 35 Å/(2-Å Hf + 4-Å Al) + oxide/CoFe 35 Å/Ti 50 Å. The barrier was oxidized for 5 min at 1 torr, and the sample was annealed at 240 °C for 40 min. Both as-deposited and annealed samples were analyzed. Fig. 4(a) shows the XPS spectra for the Hf 4f core level after ion milling to the depth where the maximum HfO_x signal appeared. The metallic Hf contribution should appear at 14.1–14.5 eV (4f7/2) and 15.8–16.2 eV (4f5/2), while HfO_2 should appear at 16.5–17 eV (4f7/2) and 18.7–19 eV (4f5/2). From the

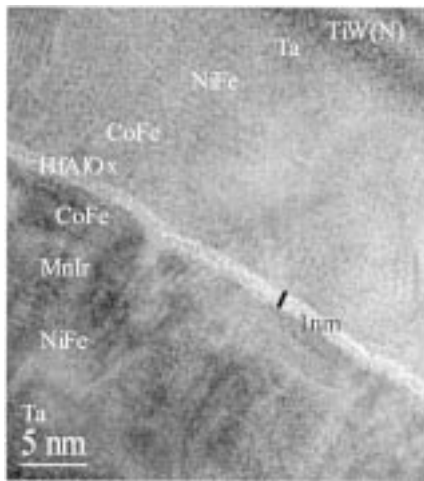


Fig. 3. High-resolution TEM micrograph showing the stacking sequence of the junction and the amorphous HfAlO_x barrier.

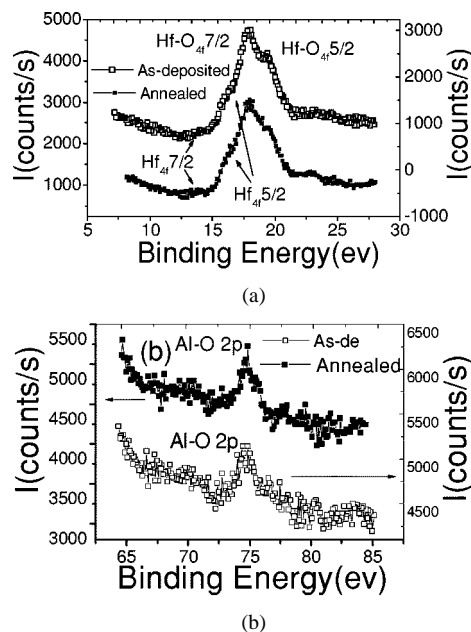


Fig. 4. XPS spectra. (a) Hf and HfO_2 . (b) AlO_x .

spectra, there is still a small amount of nonoxidized metallic Hf left in the barrier close to the bottom electrode, both in the as-deposited sample (estimated 4.5% left of Hf not oxidized,

and for annealed sample, estimated 2.5% of total Hf remaining nonoxidized by fitting). This small amount of metallic Hf left in the barrier contributes to the lower TMR in these junctions. Fig. 4(b) shows the XPS spectra for AlO_x . No metallic Al is found.

IV. CONCLUSION

In conclusion, low-resistance tunnel junctions with HfAlO_x barriers have been fabricated. The inclusion of Hf inside the barrier has helped to provide continuous and amorphous barriers that follow conformally the bottom electrode topography. $R \times A$ products below $1 \Omega \times \mu\text{m}^2$ were achieved for junction with $(2\text{-}\text{\AA} \text{ Hf} + 3\text{-}\text{\AA} \text{ Al}) + \text{oxide barriers}$ with 9.5% TMR signals. It was shown that a significant effect of current inhomogeneity exists, reducing the measured TMR and increasing measured $R \times A$ values on the measured $1 \mu\text{m}^2$ junctions. XPS analysis indicates about 2.5% of metallic Hf left unoxidized. These junctions are a good candidate for read-head applications.

REFERENCES

- [1] J. J. Sun, N. Kasahara, K. Sato, K. Shimazawa, S. Araki, and M. Matsuzaki, "Magnetic tunnel junctions on magnetic shield smoothed by gas cluster ion beam," *J. Appl. Phys.*, vol. 89, pp. 6653–6655, June 2001.
- [2] D. Song, J. Nowak, R. Larson, P. Kolbo, and R. Chellew, "Demonstrating a tunneling magnetoresistive read head," *IEEE Trans. Magn.*, vol. 36, pp. 2545–2548, Sept. 2000.
- [3] P. P. Freitas, S. Cardoso, R. C. Sousa, W. Ku, R. Ferreira, V. Chu, and J. P. Conde, "Spin dependent tunnel junctions for memory and read-head applications," *IEEE Trans. Magn.*, vol. 36, pp. 2796–2801, Sept. 2000.
- [4] Z. G. Zhang, P. P. Freitas, A. R. Ramos, N. P. Barradas, and J. C. Soares, "Resistance decrease in spin tunnel junction by control of natural oxidation condition," *Appl. Phys. Lett.*, vol. 79, pp. 2219–2221, Oct. 2001.
- [5] J. Wang, P. P. Freitas, and E. Snoeck, "Low resistance spin-dependent tunnel junctions with ZrAlO_x barriers," *Appl. Phys. Lett.*, vol. 79, pp. 4553–4555, Dec. 2001.
- [6] H. Li, Z. Wang, P. P. Freitas, J. B. Sousa, P. Gogol, and J. Chapman, "Exchange enhancement and thermal anneal in Mn_7Ir_2 bottom-pinned spin valves," *J. Appl. Phys.*, vol. 89, pp. 6904–6906, June 2001.
- [7] J. S. Moodera, L. R. Kinder, J. Nowak, P. LeClair, and R. Meservy, "Geometrically enhanced magnetoresistance in ferromagnet-insulator-ferromagnet tunnel junctions," *Appl. Phys. Lett.*, vol. 69, pp. 708–710, 1996.
- [8] K. Matsuda, N. Watari, A. Kamijo, and H. Tsuge, "Reduced magnetoresistance in magnetic tunnel junctions caused by geometrical artifacts," *Appl. Phys. Lett.*, vol. 77, pp. 3060–3062, 2000.
- [9] J. Chen, Y. Li, J. Nowak, and J. Fernandez-de-Castro, "An analytical method for 2D current crowding effect in magnetic tunnel junctions," *J. Appl. Phys.*, vol. 91, pp. 8783–8785, May 2002.
- [10] M. Kamon, M. J. Tsuk, and J. White, "FASTHENRY: A multipole-accelerated 3-D inductance extraction program," *IEEE Trans. Microwave Theory Tech.*, vol. 42, pp. 1750–1758, Sept. 1994.